www.elsevier.nl/locate/jorganchem
Journal of Organometallic Chemistry 611 (2000) 280–287

An ab initio study on the structure and reactivity of 1,4-disilabenzene

Song-Yun Kang [a], Kazunari Yoshizawa [a,*], Tokio Yamabe [b], Akinobu Naka [c], Mitsuo Ishikawa [c]

[a] *Department of Molecular Engineering, Kyoto University, Sakyo-ku, Kyoto 606-8501, Japan*
[b] *Institute for Fundamental Chemistry, 34-4 Takano-Nishihiraki-cho, Sakyo-ku, Kyoto 606-8103, Japan*
[c] *Department of Chemical Technology, Kurashiki University of Science and the Arts, 2640 Nishinoura, Tsurajima-cho, Kurashiki, Okayama 712-8505, Japan*

Received 24 February 2000; accepted 30 March 2000

Abstract

Possible reaction pathways for the conversion of Dewar-type 1,4-disilabenzene (**1**) to 1,4-disilabenzene (**2**) are discussed by means of B3LYP/6-31G** density functional theory and multiconfigurational CASSCF(6,6)/6-31G** calculations. The activation energy for the symmetry-allowed conrotatory ring opening of **1** is 34.6 kcal mol^{-1} at the B3LYP level and 47.7 kcal mol^{-1} at the CASSCF level, and that for the symmetry-forbidden disrotatory ring opening is 36.6 kcal mol^{-1} and 54.3 kcal mol^{-1} at the same levels. In both calculations the conrotatory ring opening of **1** proceeds through a potential energy barrier that is 2.0–6.6 kcal mol^{-1} lower than that of the disrotatory ring opening. Thus, we conclude that the conrotatory pathway is energetically more preferred than the disrotatory pathway. The Diels–Alder reaction of 1,4-disilabenzene and acetylene is also discussed. The activation energy for the Diels–Alder addition is computed to be 4.2 kcal mol^{-1} at the B3LYP/6-31G** level. Thus, 1,4-disilabenzene is highly reactive, and once 1,4-disilabenzenes are produced, the Diels–Alder additions of 1,4-disilabenzenes with many kinds of dienophiles should readily take place. © 2000 Elsevier Science S.A. All rights reserved.

Keywords: 1,4-Disilabenzenes; Dewar-type; Diels–Alder reaction; Density functional theory

1. Introduction

The synthesis and isolation of compounds having multiple bonds to silicon have been one of the major challenges in main group chemistry [1,2]. The first stable compounds with double bonds to silicon were synthesized in 1981 [3,4], and since then this group of compounds has been studied extensively [5]. Aromatic compounds containing silicon have also attracted considerable interest, both experimentally [6–27] and theoretically [28–37], and efforts in this area have been intensified since the first synthesis of stable silenes and disilenes. Silabenzene and 1-methylsilabenzene have been identified by means of IR-, UV-, and PE-spectroscopies in an argon matrix at 10 K [10–12]. 1-{2,4,6-Tris[bis(trimethylsilyl)methyl]phenyl}-silabenzene was recently isolated in C_6D_6 by Wakita, Okazaki, and coworkers [27]. Moreover, Dewar-type 1,4-disilabenzene was synthesized following Scheme 1 and characterized from an X-ray diffraction analysis by Kabe, Ando, and coworkers [38]. 1,4-Disilabenzenes are unstable in general, but can be detected by trapping the reactions with hexafluoro-2-butyne or acetylene that produces 1,4-disilabarrelenes [15,21], as indicated in Scheme 2.

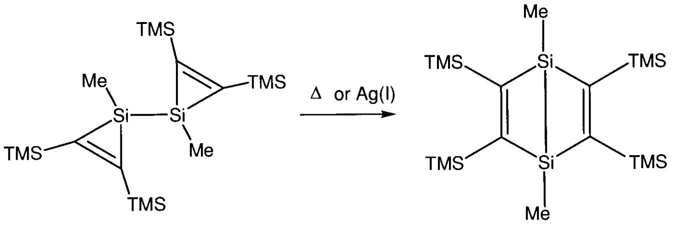

Scheme 1.

---

* Corresponding author. Tel.: +81-75-753-5932; fax: +81-75-751-7279.

E-mail address: kazunari@scl.kyoto-u.ac.jp (K. Yoshizawa).

PII: S0022-328X(00)00495-2

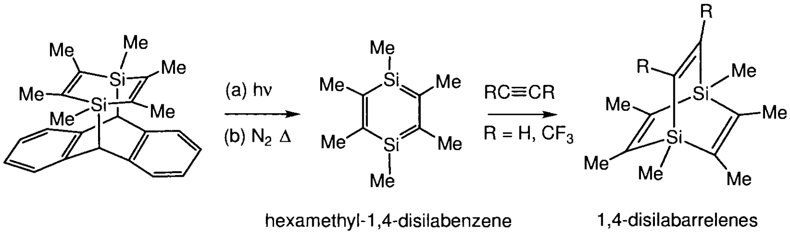

Scheme 2.

Our knowledge of these silicon compounds can be derived from quantum chemical calculations as one of the main sources of reliable information. Chandrasekhar and Schleyer discussed the possibility of a photochemical valence isomerization of disilabenzene to Dewar-type disilabenzene from ab initio calculations [34]. Their Hartree–Fock (HF) calculations tell us that disilabenzene should be more stable than its Dewar form by 10.7 kcal mol^{-1} at the HF/STO-3G level and 5.9 kcal mol^{-1} at the HF/3-21G* level, and more recent calculations by Ando et al. [39] afforded 2.3 kcal mol^{-1} for the same quantity at the HF/6-31G* level of theory. This result is due to reduced aromaticity in 1,4-disilabenzene as well as to the greater strength of the Si–Si σ bonds and the C=C double bonds in the Dewar form.

We report here our results of ab initio investigations on the chemistry outlined in Scheme 3. Our results include a theoretical prediction for the reaction pathway from Dewar-type 1,4-disilabenzene to 1,4-disilabenzene, which involves two types of transition states; one is a symmetry-allowed conrotatory ring opening, and the other is a symmetry-forbidden disrotatory ring opening. The Woodward–Hoffmann rules [40,41] tell us from orbital symmetry relationships that in the carbon system cyclobutene is smoothly transformed into butadiene in a conrotatory process by heat treatment. Johnson and Daust [42] indicated that Dewar benzene lies 77.8 kcal mol^{-1} above benzene and that the conrotatory ring opening of Dewar benzene to benzene should take place through the transition state for the conrotatory ring opening, which lies 3.7 kcal mol^{-1} below that for the disrotatory ring opening at the MP4//MP2/6-31G* level of theory. Therefore it is of great interest to study the stereochemistry and energetics of the ring opening process of Dewar-type 1,4-disilabenzene. The main purpose of this work is to investigate which pathway is energetically more reasonable for the conversion of the Dewar form to the benzene form. We also study the reactivity of 1,4-disilabenzene through computing the reaction of 1,4-disilabenzene and acetylene.

2. Method of calculation

We calculated the reaction pathways indicated in Scheme 3. Detailed analyses for the reactants, products, and transition states (TSs) and the intrinsic reaction coordinate (IRC) [43,44] that connects these reaction species were carried out using a hybrid Hartree–Fock/density-functional-theory (HF/DFT) method (the so-called B3LYP method) [45–47]. This method consists of the nonlocal exchange functional of Becke's three-parameter set [45,46] and the nonlocal correlation functional of Lee, Yang, and Parr [47]. It has been successfully applied to the Diels–Alder reaction of butadiene and ethylene [48], providing better results than the Møller–Plesset (MP) perturbation theory method, concerning molecular structures and energetics. IRC was traced from a transition state toward both Dewar-type 1,4-disilabenzene and 1,4-disilabenzene directions along the imaginary mode of vibration using the algorithm developed by Gonzalez and Schlegel [49] in the mass-weighted internal coordinate system. IRC was

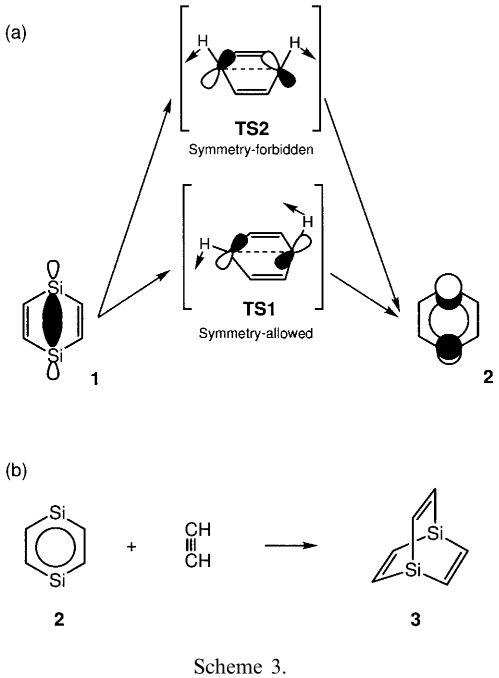

Scheme 3.

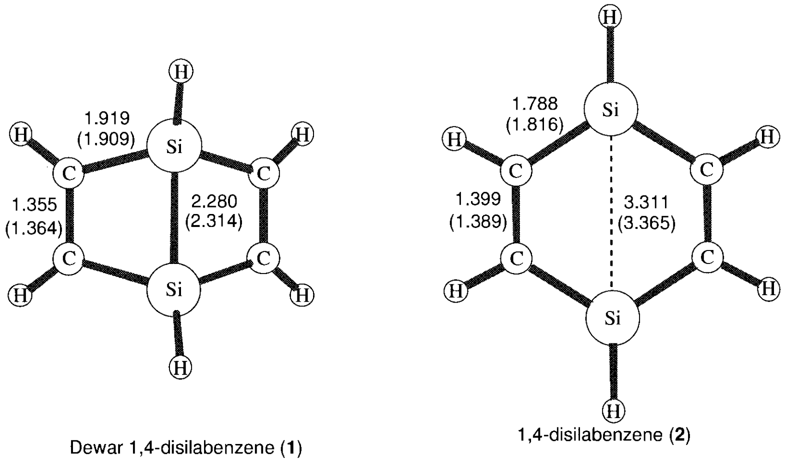

Fig. 1. Optimized geometries of Dewar-type 1,4-disilabenzene (**1**) and 1,4-disilabenzene (**2**) at the B3LYP/6-31G** level and the CASSCF(6,6)/6-31G** level (indicated in parentheses). Bond distances are in Å.

constructed from a total of 100 steps to an accuracy of 0.1 amu$^{1/2}$ bohr of s, in which s is the length of IRC. Multiconfigurational CASSCF (complete active space self-consistent field) calculations [50,51] were also carried out using the six-electron-six-orbital (6,6) active space involving the π-orbitals of 1,4-disilabenzene. We used the 6-31G** basis set, a standard double-ζ basis set with polarization functions [52–54]. Vibrational mode analyses were systematically carried out to confirm that on potential energy surfaces optimized geometries correspond to a local minimum that has no imaginary frequency mode or a saddle point that has only one imaginary mode. Corrections of zero-point vibrational energies were taken into account in all stationary structures thus obtained. The GAUSSIAN-98 ab initio program was used throughout this work [55].

3. Results and discussion

3.1. Electrocyclic ring opening of Dewar-type 1,4-disilabenzene

We first calculated the conversion of Dewar-type 1,4-disilabenzene (1,4-disilabicyclo[2.2.0]hexa-2,5-diene (**1**)) to 1,4-disilabenzene (**2**). Optimized structures of **1** and **2** at the B3LYP level are shown in Fig. 1. The larger balls stand for silicon atoms, and the smaller balls carbon atoms. Computed total energies and zero-point vibrational energies are summarized in Table 1.

Kabe et al. [38] recently performed an X-ray structural analysis of a Dewar-type 1,4-disilabenzene; the Si–Si distance is 2.247 Å, the four Si–C distances are in a range 1.921–1.939 Å, and the two C–C distances are 1.386 and 1.379 Å. Our computational results for **1** indicated in Fig. 1 are in excellent agreement with the X-ray structure of the Dewar-type 1,4-disilabenzene. The Si–C bond lengths (1.788 Å) in **2** lie between those of Si–C single (1.885 Å [26]) and double bonds (1.708 Å [26]), and the C–C bond lengths (1.399) in **2** are in excellent agreement with the C–C bond lengths (1.395 Å) in aromatic compounds [56]. At the B3LYP level, **1** was predicted to lie 14.4 kcal mol^{-1} above **2**, thus the energetical stability of the benzene form being significantly reduced in the silicon compound.

Two possible transition states for the ring opening were found at the B3LYP level of theory. As indicated in Scheme 3, there are two reaction pathways for the conversion of **1** to **2**; one is the symmetry-allowed conrotatory pathway (**TS1**), and the other is the symmetry-forbidden disrotatory pathway (**TS2**). Fig. 2a shows the saddle-point structure for **TS1** as well as the imaginary vibrational mode that clearly corresponds to the conrotatory electronic process upon cleavage of the Si–Si σ bond. On the other hand, our vibrational analysis for **TS2** at the B3LYP/6-31G** level resulted

Table 1
Total energies for the reaction species and the transition states at the B3LYP/6-31G** level and the CASSCF(6,6)/6-31G** level [a]

	B3LYP/6-31G**		CASSCF/6-31G**	
	Energy (au)	ZPE (kcal mol^{-1})	Energy (au)	ZPE (kcal mol^{-1})
Acetylene	−77.32957	16.8		
1	−734.93018	51.2	−732.77106	54.0
TS1	−734.87162	49.1	−732.69277	52.6
TS2	−734.86927 [b]	49.6 [b]	−732.68491	54.2
2	−734.95324	51.3	−732.77828	53.6
TS3	−812.27689	68.6		
3	−812.38934	72.4		

[a] ZPE is zero-point vibrational energy. au = 27.21 eV = 627.5 kcal mol^{-1}.

[b] Second-order saddle point.

(a) **TS1**

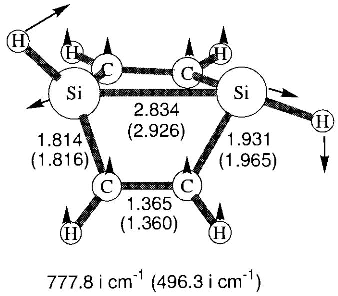

(b) **TS2**

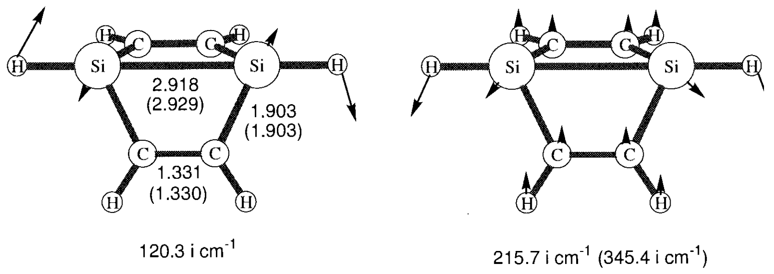

Fig. 2. Optimized geometries of **TS1** and **TS2** at the B3LYP/6-31G** level and the CASSCF(6,6)/6-31G** level (indicated in parentheses). The B3LYP method gives two imaginary modes for **TS2**. Bond lengths are in Å.

in two imaginary modes, which suggests this structure to be a second-order (or so-called monkey) saddle point. Fig. 2b shows the two imaginary vibrational modes for **TS2**. Similar observations of second-order saddle points have been made for the disrotatory ring opening of cyclobutene [57] and the [$\pi 2s + \pi 2s$] dimerization of ethylene [58,59]. Thus, such a case may occur frequently for symmetry-forbidden electronic processes. In Fig. 2b, the high-frequency mode correctly corresponds to the disrotatory ring opening, while the low-frequency mode leads to the distortion back to the conrotatory pathway that is the true transition state from the viewpoint that it has a single imaginary mode. The activation energy for **TS1** was predicted to be 34.6 kcal mol^{-1} and that for **TS2** 36.6 kcal mol^{-1} at the B3LYP/6-31G** level, as shown in Fig. 3, thus the activation energy for **TS1** being slightly lower than that for **TS2**. Kabe et al. recently reported that the activation energy for the conversion of 1 to 2 is 105 kcal mol^{-1} at the HF/6-31G* level and 144.7 kcal mol^{-1} at the MP2/6-31G* level [38], the results being quantitatively different from our B3LYP results.

In order to better understand the mechanism of the conversion of **1** to **2**, we performed an IRC analysis for the conrotatory pathway. The changes in the Si–Si, Si–C, and C–C distances along the IRC carried out at the B3LYP/6-31G** level are shown in Fig. 4. The IRC was traced from **TS1** ($s = 0$), which exhibits a C_s structure with an imaginary vibrational mode of 777.8i cm^{-1}, toward both **1** ($s < 0$) and **2** ($s > 0$) directions. The r_1 and r_2 represent the shorter Si–C distance and the longer Si–C distance in **TS1**, respectively. Starting from **1** the Si–Si distance gradually increases and finally the Si–Si bond is cleaved. The C–C distance slowly increases and after passing **TS1** it starts to significantly increase. In fact, the C–C distance of 1.365 Å in **TS1** is only 0.01 Å longer than that of **1**. In contrast, the r_1 and r_2 are significantly changed along the reaction coordinate, leading to the formation of the Si–C aromatic bonds.

The energy profile along the IRC is shown in Fig. 5. The relative energies are measured from the total energy of **1**. This result clearly demonstrates that **TS1** is the true transition state for the conversion of **1** to **2** via the symmetry-allowed conrotatory electronic process.

To confirm that our results presented above are not an artifact of the B3LYP methodology, further multiconfigurational CASSCF(6,6)/6-31G** calculations were carried out. The optimized geometries for the stable structures and the transition states are shown in Figs. 1 and 2, respectively. Computed total energies and zero-point vibrational energies are summarized in Table 1. The energies and geometries are in fairly good agreement with the B3LYP predictions in general. At the CASSCF level, **1** was predicted to be 4.9 kcal mol^{-1} above **2**. Although the Si–Si–H angle in **2** is changed from 180° at the B3LYP level to 154.4° at the CASSCF level, other geometrical parameters are almost identical in both methodologies. The activation energy for **TS1** was predicted to be 47.7 kcal mol^{-1} and that for **TS2** 54.3 kcal mol^{-1} at the CASSCF level. At the CASSCF level **TS2** was confirmed to correctly have only one imaginary frequency. In both methodologies the conrotatory process via **TS1** lies lower in energy than the disrotatory process via **TS2**.

3.2. Diels–Alder reaction of 1,4-disilabenzene and acetylene

Having described the ring-opening reactions of Dewar-type 1,4-disilabenzene (**1**) to 1,4-disilabenzene (**2**), we next address the Diels–Alder reaction of **2** and acetylene. A computed potential energy profile, including zero-point energy corrections, along the concerted reaction pathway for the addition of **2** and acetylene at the B3LYP level is presented in Fig. 6. The relative energies indicated are measured from the dissociation limit of **2** and acetylene.

The transition state (**TS3**) in this illustration is concerned with the concerted Diels–Alder reaction of **2** and acetylene. The activation energy for **TS3** was predicted to be 4.2 kcal mol^{-1}; we thus expect that this reaction should readily take place if **2** is produced. Since the product of this reaction, 1,4-disilabarrelene (1,4-disilabicyclo[2.2.2]octa-2,5,7-triene, **3**), lies 62.6 kcal mol^{-1} below the reactants, this electronic process is considered to be irreversible. The reactivity of **2** is so high that the activation energy of this Diels–Alder reaction is much smaller than those of the well-characterized Diels–Alder reactions of butadiene and ethylene (24.8 kcal mol^{-1} at the B3LYP/6-31G* level [48]) and of butadiene and acetylene (25.0 kcal mol^{-1} at the B3LYP/6-31G* level [60]). It is slightly higher than the activation energy of the Diels–Alder reaction of 1,4-disilabutadiene and acetylene (0.9 kcal mol^{-1} at the B3LYP/6-31G** level [61]). Fig. 6 also shows optimized geometries of the reaction species along the reaction pathway. Sekiguchi, Gillette, and West [21] performed an X-ray structural analysis of 1,4-dimethyl-2,3,5,6,7,8-tetraphenyl-1,4-disilabarrelene; the Si–C distances lie in a range of 1.886–1.905 Å, the C–C distances lie in a range of 1.334–1.367 Å, and the Si–Si non-bonded distance is 2.93 Å. Our computational results for **3** indicated in Fig. 6 are in excellent agreement with the X-ray structural analysis of this 1,4-disilabarrelene. The transition state **TS3** conserves C_{2v} symmetry, and therefore it is symmetrical with respect to the Si–C bonds being formed. These Si–C bonds are predicted to be 2.921 Å in length, which is reasonably about 1.5 times as long as the Si–C bond distances of organosilicon compounds. The arrows in **TS3** indicate the imaginary vibrational mode of $227.9i_{+}$ cm^{-1}; this transition vector is of course symmetrical and conserves C_{2v} symme-

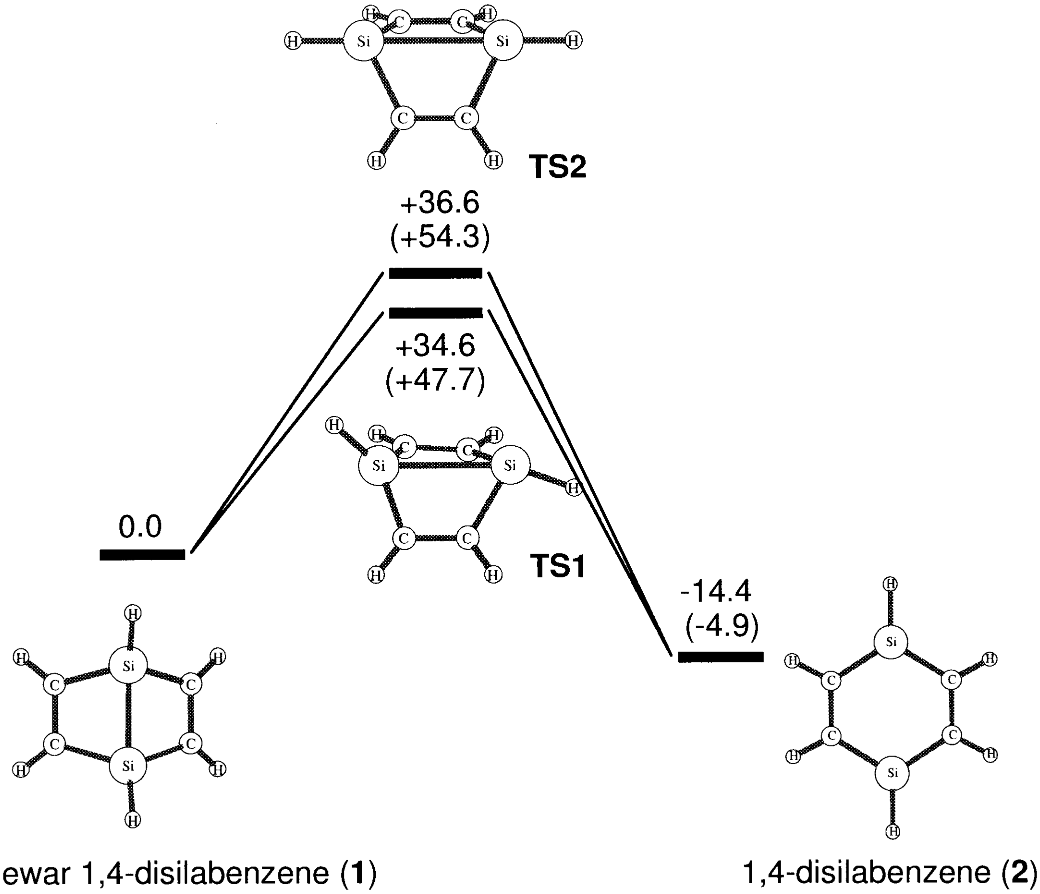

Fig. 3. Potential energy diagram for the reaction of Dewar-type 1,4-disilabenzene (**1**) to 1.4-disilabenzene (**2**) at the B3LYP/6-31G** level, and at the CASSCF(6,6)/6-31G** level (indicated in parentheses). Relative energies are in kcal mol^{-1}.

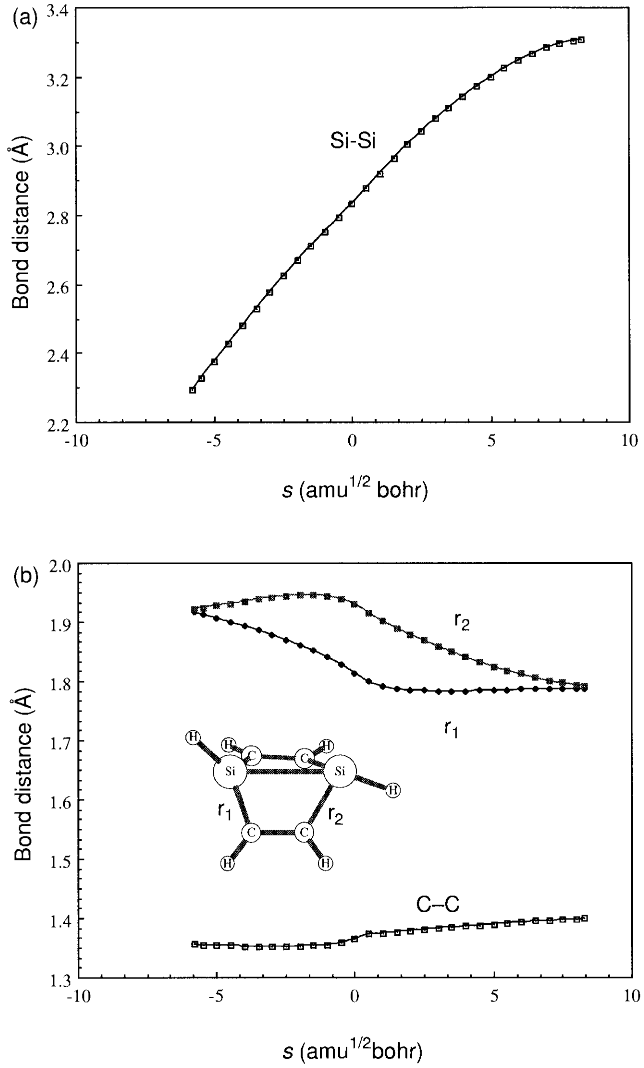

Fig. 4. Changes of internal coordinates along the IRC.

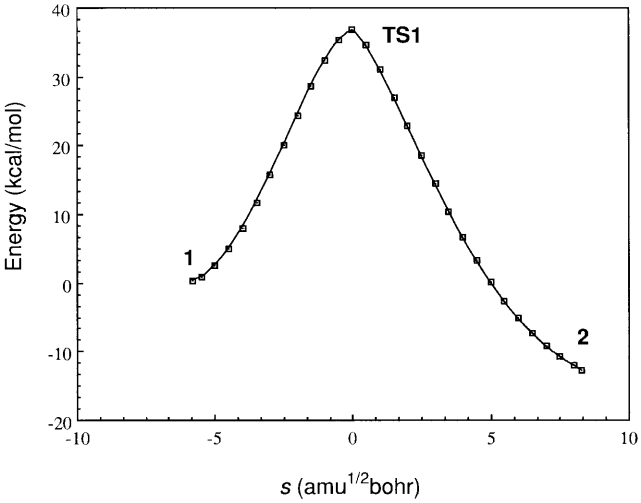

Fig. 5. Potential energy along the IRC from **1** to **2**.

try, suggesting preferred nuclear motions along the reaction coordinate. Thus, the transition-state structure is quite appropriate for this synchronous concerted reaction.

The energy levels of the π orbitals of benzene and **2** calculated at the B3LYP/6-31G** level is shown in Fig. 7. Benzene has a D_{6h} geometry and its π-HOMO and π*-LUMO are doubly generate. On the other hand, **2** is distorted to a D_{2h} geometry and as a result the orbital degeneracy is removed; one member of the π-HOMO increases in energy from −6.719 eV (e_{1g}) to −5.037 eV (b_{2g}), and the other decreases in energy to −7.297 eV (b_{1g}), as indicated. The degenerate π*-LUMO decreases in energy from +0.072 eV (e_{2u}) to −0.809 eV (a_u) and −1.143 eV (b_{3u}). These orbital splittings are the main reason for the high reactivity of 1,4-disilabenzenes. When the Diels–Alder reaction between **2** and acetylene occurs, the b_{2g} HOMO and the b_{3u} LUMO of **2** play an important role. The orbital amplitude of these frontier orbitals is significantly located on the silicon atoms, while in benzene one member of the degenerate HOMO and LUMO has no orbital amplitude on the 1- and 4-site carbons. Therefore the orbital interaction between the HOMO of **2** and the LUMO of acetylene and that between the LUMO of **2** and the HOMO of acetylene get stronger in 1,4-disilabenzene. It is clear that the high-lying HOMO and the low-lying LUMO make this silicon compound very reactive.

4. Concluding remarks

We have discussed the conversion of Dewar-type 1,4-disilabenzene (**1**) to 1,4-disilabenzene (**2**) from both B3LYP DFT calculations and CASSCF calculations and the Diels–Alder reaction of **2** and acetylene from B3LYP calculations. Detailed descriptions on the total energies of the reaction species (stable points) and the transition states (saddle points) investigated in this work are listed in Table 1. We compared the energetics of the conrotatory and disrotatory electronic processes for the conversion of **1** to **2**. The activation energy for the symmetry-allowed conrotatory ring opening of **1** is 34.6 kcal mol^{-1} at the B3LYP level and 47.7 kcal mol^{-1} at the CASSCF level, and that for the symme-try-forbidden disrotatory ring opening of **1** is 36.6 kcal mol^{-1} and 54.3 kcal mol^{-1} at the same levels. In both calculations the conrotatory ring opening of **1** proceeds through a barrier that is 2.0–6.6 kcal mol^{-1} lower than that of the disrotatory ring opening. Thus, we concluded that the conrotatory pathway is energetically more preferred than the disrotatory pathway. The activation energy for the Diels–Alder reaction of **2** and acetylene is 4.2 kcal mol^{-1} at the B3LYP level. Therefore once **2** is produced, coupling reactions of **2** with many kinds of dienophiles are expected to readily take place. This is why 1,4-disilabenzenes are unstable and difficult to isolate.

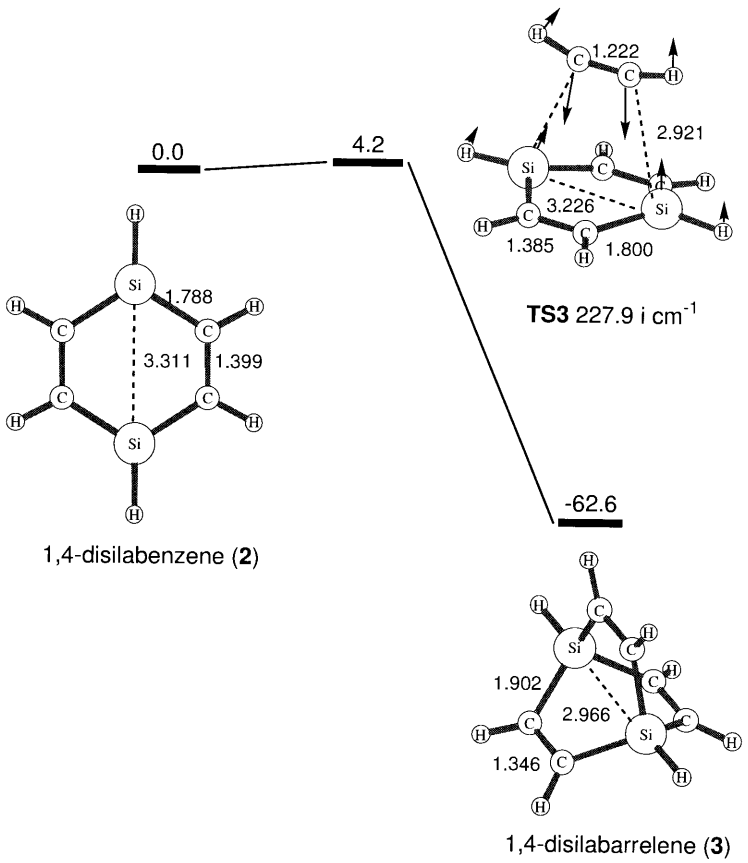

Fig. 6. Potential energy diagram for the reaction of 1,4-disilabenzene (**2**) and acetylene at the B3LYP/6-31G** level. Relative energies are in kcal mol^{-1}. Bond distances are in Å.

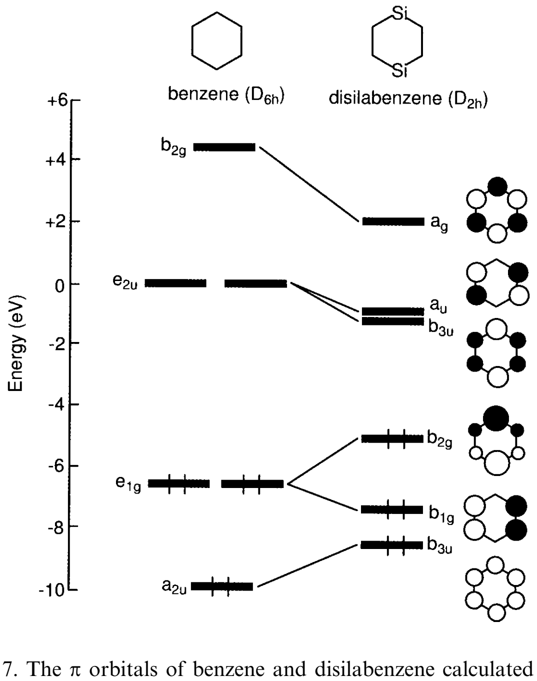

Fig. 7. The π orbitals of benzene and disilabenzene calculated at the B3LYP/6-31G** level.

Acknowledgements

We are grateful for a Grant-in-Aid for Scientific Research on the Priority Area The Chemistry of Inter-element Linkage from the Ministry of Education, Science, Sports and Culture of Japan and to the Research for the Future Program from the Japan Society for the Promotion of Science (JSPS-RFTF96P00206) for their support of this work. Computations were partly carried out at the Supercomputer Laboratory of Kyoto University and at the Computer Center of the Institute for Molecular Science.

References

[1] S. Patai, Z. Rappoport, The Chemistry of Organic Silicon Compounds, Wiley, New York, 1989.
[2] Z. Rappoport, Y. Apeloig, The Chemistry of Organic Silicon Compounds, vol. 2, Wiley, New York, 1998.
[3] A.G. Brook, F. Abdesaken, B. Gutekunst, G. Gutekunst, R.K. Kallury, J. Chem. Soc. (1981) 191.
[4] R. West, M.J. Fink, J. Michl, Science 214 (1981) 1343.
[5] G. Raabe, J. Michl, Chem. Rev. 85 (1985) 419.
[6] T.J. Barton, D.S. Banasiak, J. Am. Chem. Soc. 99 (1977) 5199.
[7] T.J. Barton, D.S. Banasiak, J. Organomet. Chem. 157 (1978) 255.

[8] T.J. Barton, G.T. Burns, J. Am. Chem. Soc. 100 (1978) 5246.
[9] G. Märkl, P. Hofmeister, Angew. Chem. Int. Ed. Engl. 18 (1979) 789.
[10] H. Bock, R.A. Bowling, B. Solouki, T.J. Barton, G.T. Burns, J. Am. Chem. Soc. 102 (1980) 429.
[11] C.L. Kreil, O.L. Chapman, G.T. Burns, T.J. Barton, J. Am. Chem. Soc. 102 (1980) 841.
[12] B. Solouki, P. Rosmus, H. Bock, G. Maier, Angew. Chem. Int. Ed. Engl. 19 (1980) 51.
[13] T.J. Barton, M. Vuper, J. Am. Chem. Soc. 103 (1981) 6788.
[14] G. Maier, G. Mihm, H.P. Reisenauer, Chem. Ber. 115 (1982) 801.
[15] J.D. Rich, R. West, J. Am. Chem. Soc. 104 (1982) 6884.
[16] W. Ando, H. Tanikawa, A. Sekiguchi, Tetra. Lett. 24 (1983) 4245.
[17] H. Bock, P. Rosmus, B. Solouki, G. Maier, J. Organomet. Chem. 271 (1984) 145.
[18] G. Maier, G. Mihm, R.O.W. Baumgärtner, H.P. Reisenauer, Chem. Ber. 117 (1984) 2337.
[19] G. Maier, K. Schöttler, H.P. Reisenauer, Tetra. Lett. 26 (1985) 4079.
[20] G. Märkl, W. Schlosser, Angew. Chem. Int. Ed. Engl. 27 (1988) 963.
[21] A. Sekiguchi, G.R. Gillette, R. West, Organometallics 7 (1988) 1226.
[22] Y.v.d. Winkel, B.L.M.v. Baar, F. Bickelhaupt, W. Kulik, C. Sierakowski, G. Maier, Chem. Ber. 124 (1991) 185.
[23] H. Hiratsuka, M. Tanaka, T. Okutsu, M. Oba, K. Nishiyama, J. Chem. Soc. Chem. Commun. (1995) 215.
[24] N. Tokitoh, K. Wakita, R. Okazaki, S. Nagase, P.v.R. Schleyer, H. Jiao, J. Am. Chem. Soc. 119 (1997) 6951.
[25] T. Müller, Angew. Chem. Int. Ed. 37 (1998) 68.
[26] K. Wakita, N. Tokitoh, R. Okazaki, S. Nagase, P.v.R. Schleyer, H. Jiao, J. Am. Chem. Soc. 121 (1999) 11336.
[27] K. Wakita, N. Tokitoh, T. Kawashima, R. Okazaki, S. Nagase, Proceedings of 76th National Meeting of the Chemical Society of Japan, Tokyo, March 1999, Abstr., No. 3B510.
[28] M.J.S. Dewar, D.H. Lo, C.A. Ramsden, J. Am. Chem. Soc. 97 (1975) 1311.
[29] H.B. Schlegel, B. Coleman, M. Jones, Jr., J. Am. Chem. Soc. 100 (1978) 6499.
[30] P.H. Blustin, J. Organomet. Chem. 166 (1979) 21.
[31] J. Chandrasekhar, P.v.R. Schleyer, R.O.W. Baumgärtner, M.T. Reetz, J. Org. Chem. 48 (1983) 3453.
[32] M.S. Gordon, P. Boudjouk, F. Anwari, J. Am. Chem. Soc. 105 (1983) 4972.
[33] K.K. Baldridge, M.S. Gordon, J. Organomet. Chem. 271 (1984) 369.
[34] J. Chandrasekhar, P.v.R. Schleyer, J. Organomet. Chem. 289 (1985) 51.
[35] K.K. Baldridge, M.S. Gordon, J. Am. Chem. Soc. 110 (1988) 4204.
[36] H.J. Hofmann, R. Cimiraglia, M. Persico, Chem. Phys. Lett. 146 (1988) 249.
[37] H. Bock, Angew. Chem. Int. Ed. Engl. 28 (1989) 1627.
[38] Y. Kabe, Proceedings of The Fifth Symposium on the Chemistry of Inter-element Linkage, Kyoto, 2000, p. 85.
[39] W. Ando, T. Shiba, T. Hidaka, K. Morihashi, O. Kikuchi, J. Am. Chem. Soc. 119 (1997) 3629.
[40] R. Hoffmann, R.B. Woodward, J. Am. Chem. Soc. 87 (1965) 2046.
[41] R.B. Woodward, R. Hoffmann, The Conservation of Orbital Symmetry, Verlag, Weinheim, 1970.
[42] R.P. Johnson, K.J. Daoust, J. Am. Chem. Soc. 118 (1996) 7381.
[43] K. Fukui, J. Phys. Chem. 74 (1970) 4161.
[44] K. Fukui, Acc. Chem. Res. 14 (1981) 363.
[45] A.D. Becke, Phys. Rev., Sect. A 38 (1988) 3098.
[46] A.D. Becke, J. Chem. Phys. 98 (1993) 5648.
[47] C. Lee, W. Yang, R.G. Parr, Phys. Rev. Sect. B 37 (1988) 785.
[48] E. Goldstein, B. Beno, K.N. Houk, J. Am. Chem. Soc. 118 (1996) 6036.
[49] C. Gonzalez, H.B. Schlegel, J. Phys. Chem. 94 (1990) 5523.
[50] D. Hegarty, M.A. Robb, Mol. Phys. 38 (1979) 1795.
[51] R.H.E. Eade, M.A. Robb, Chem. Phys. Lett. 83 (1981) 362.
[52] W.J. Hehre, R. Ditchfield, J.A. Pople, J. Chem. Phys. 56 (1972) 2257.
[53] P.C. Hariharan, J.A. Pople, Theor. Chim. Acta 28 (1973) 213.
[54] M.S. Gordon, Chem. Phys. Lett. 76 (1980) 163.
[55] M.J. Frisch, G.W. Trucks, H.B. Schlegel, G.E. Scuseria, M.A. Robb, J.R. Cheeseman, V.G. Zakrzewski, J.A. Montgomery, R.E. Stratmann, J.C. Burant, S. Dapprich, J.M. Millam, A.D. Daniels, K.N. Kudin, M.C. Strain, O. Farkas, J. Tomasi, V. Barone, M. Cossi, R. Cammi, B. Mennucci, C. Pomelli, C. Adamo, S. Clifford, J. Ochterski, G.A. Petersson, P.Y. Ayala, Q. Cui, K. Morokuma, D.K. Malick, A.D. Rabuck, K. Raghavachari, J.B. Foresman, J. Cioslowski, J.V. Ortiz, B.B. Stefanov, G. Liu, A. Liashenko, P. Piskorz, I. Komaromi, R. Gomperts, R.L. Martin, D.J. Fox, T. Keith, M.A. Al-Laham, C.Y. Peng, A. Nanayakkara, C. Gonzalez, M. Challacombe, P.M.W. Gill, B.G. Johnson, W. Chen, M.W. Wong, J.L. Andres, M. Head-Gordon, E.S. Replogle, J.A. Pople, GAUSSIAN-98, Gaussian, Pittsburgh, PA, 1998.
[56] D.R. Lide, CRC Handbook of Chemistry and Physics, 67, CRC Press, New York, 1986–1987.
[57] J. Breulet, H.F. Schaefer III, J. Am. Chem. Soc. 106 (1984) 1221.
[58] F. Bernardi, A. Bottoni, M.A. Robb, H.B. Schlegel, G. Tonachini, J. Am. Chem. Soc. 107 (1985) 2260.
[59] F. Bernardi, P. Celani, M. Olivucci, M.A. Robb, G. Suzzi-Valli, J. Am. Chem. Soc. 117 (1995) 10531.
[60] R.D.J. Froese, J.M. Coxon, S.C. West, K. Morokuma, J. Org. Chem. 62 (1997) 6991.
[61] K. Yoshizawa, S.Y. Kang, T. Yamabe, A. Naka, M. Ishikawa, Organometallics 18 (1999) 4637.